Asian Journal of Chemistry; Vol. 29, No. 12 (2017), 2717-2724
ASIAN JOURNAL OF CHEMISTRY
https://doi.org/10.14233/ajchem.2017.20841

Spectroscopic Analysis and Computational Investigation (FMO, MESP and NLO) of 1,2-Dimethylnaphthalene

E. JAYACHITHRA[1,*] and R. MADIVANANE[2]

[1]Department of Physics, Research and Development Center, Bharathiar University, Coimbatore-641 046, India
[2]Department of Physics, Mahatma Gandhi Arts and Science College, Mahe-673 311, India

*Corresponding author: E-mail: jc.chitraphy@gmail.com

Received: 5 June 2017; *Accepted*: 28 July 2017; *Published online*: 30 October 2017; AJC-18622

In present study, the complete vibrational analysis of 1,2-dimethylnaphthalene has been carried out by DFT B3LYP/6-311++G basis set and HF with the same basis set. The vibrational frequencies of the optimized geometry of the molecule has been calculated and compared with the reported experimental (FT-IR, FT-Raman) values. The calculated vibrational frequencies has been scaled with multiple scale factors and it shows good agreement with the experimental spectra. Frontier molecular orbital analysis shows the occurrence of charge transfer within the molecule. The molecular electrostatic potential energy surface were plotted to understand the charge distribution within the molecule. The calculated polarizability and first order hyperpolarizability revealed that the molecule is a non-linear optical material. The thermodynamic properties of 1,2-dimethylnaphthalene are also calculated and reported in gas phase at different temperatures.

Keywords: 1,2-Dimethylnaphthalene, Vibrational spectra, DFT, Frontier molecular orbital, NLO.

INTRODUCTION

Naphthalene is a simplest polyaromatic hydrocarbon, consist of a fused pair benzene rings which is a white crystalline volatile solid with a characteristic odour of coal-tar and the most familiar household fumigant. Fossil fuels such as petroleum and coal naturally contains naphthalene [1]. Naphthalene and its derivatives are biologically, industrially and pharmaceutically significant compound [2]. Although there are many derivatives in dimethylnaphthalene, one of its derivatives 1,2-dimethylnaphthalene attracts the attention due to its wide applications. It is most commonly used in moth repellents such as moth balls and also used to make tanning agents, resins, lubricants, plastics, antiseptics, toilet deodorants and in other insecticides [3]. Even though 1,2-dimethylnaphthalene has extensive applications, neither quantum chemical calculations nor the vibrational analysis of the compound is reported in the literature, thus we recorded the vibrational spectrum and carried out the quantum chemical computations of 1,2-dimethylnaphthalene.

EXPERIMENTAL

1,2-Dimethylnaphthalene was purchased from Sigma-Aldrich Chemicals USA, with a spectroscopic grade (98 %) which was used as such without any further purification. Using Bruker IFS-66V Fourier transform spectrometer, at room temperature, Fourier transform IR spectra of the title compound, was measured at 4000-400 cm^{-1} region at a resolution of ± 2 cm^{-1}. The same instrument equipped with a FRA-106 FT Raman accessory was used to record the FT-Raman spectrum of 1,2-dimethylnaphthalene and it was recorded in the 3500-100 cm^{-1} with Nd:YAG laser operating at 200 mW power. The reported wave numbers are expected to be accurate within ± 2cm^{-1}.

Computational details: Density functional theoretical (DFT) computations have been performed at the Becke-3-Lee-Yang-Parr (B3LYP) functional [4,5] with the basis set of 6-311++G and Hatree Fock (HF) computations with the same basis set to carry out the vibrational analysis of normal modes of dimethylnaphthalene using Gaussian 09W program package [6].The molecular geometries were completely optimized and found to be the minimum energy conformer. The optimized structural parameters of 1,2-dimethylnaphthalene were used for harmonic vibrational frequency calculations resulting in IR and Raman frequencies together with intensities and Raman depolarization ratios. To compensate the errors arising from basis set incompleteness and to neglect the vibrational anharmonicity, the frequencies are scaled with multiple scale factors [7]. The animation option on the Gauss view 05 graphical interface of the Gaussian program was employed to visualize the vibrations and for proper assignment of the pure and mixed modes of 1,2-dimethylnaphthalene.

RESULTS AND DISCUSSION

Analysis of minimum energy structure: The optimized structure of compound 1,2-dimethylnaphthalene using DFT/B3LYP method with the numbering scheme is depicted in Fig. 1 and the corresponding parameters such as bond length and bond angle are presented in Table-1.

Through the minimum energy conformational analysis, it can be found that the bond length of all C=C are 1.36 Å and C-C are 1.42 Å in the naphthalene ring. The variation in the bond length between C=C and C-C suggesting that some localization of the double bonds in the ring and also due to the fact that the bond length decreases with increase in bond multiplicity, *i.e.* the electron density is greater in double bond than

TABLE-1
OPTIMIZED STRUCTURAL PARAMETERS CALCULATED FOR 1,2-DIMETHYLNAPHTHALENE

Bond length (Å)		Bond angle (°)		Dihedral angle (°)	
C1-C2	1.3934	C2-C1-C6	119.5153	C6-C1-C2-C3	-0.0002
C1-C6	1.4244	C2-C1-C17	122.3985	C6-C1-C2-C18	-180.003
C1-C17	1.5164	C6-C1-C17	118.0862	C17-C1-C2-C3	180.0012
C2-C3	1.4385	C1-C2-C3	119.6564	C17-C1-C2-C18	-0.0016
C2-C18	1.5144	C1-C2-C18	121.3467	C2-C1-C6-C5	0.0018
C3-C4	1.436	C3-C2-C18	118.9969	C2-C1-C6-H11	-179.9996
C3-C8	1.4266	C3-C2-C4	119.8435	C17-C1-C6-C5	-179.9996
C4-C5	1.4201	C2-C3-C8	122.4093	C17-C1-C6-H11	-0.0009
C4-C9	1.4231	C4-C3-C8	117.7471	C2-C1-C17-H19	179.9921
C5-C6	1.3736	C3-C4-C5	118.7853	C2-C1-C17-H20	60.3323
C5-H10	1.0834	C3-C4-C9	119.49	C2-C1-C17-H21	-60.3416
C6-H11	1.0832	C5-C4-C9	121.7248	C6-C1-C17-H19	-0.0065
C8-H7	1.0806	C5-C4-C6	120.3659	C6-C1-C17-H20	-119.6663
C8-C13	1.3798	C4-C5-H10	119.1029	C6-C1-C17-H21	119.6598
C9-C12	1.3777	C6-C5-H10	120.5311	C1-C2-C3-C4	-0.0008
C9-H14	1.0836	C1-C6-C5	121.8336	C1-C2-C3-C8	-180.0018
C12-C13	1.4163	C1-C6-H11	118.4528	C18-C2-C3-C4	180.0019
C12-H15	1.0823	C5-C6-H11	119.7136	C18-C2-C3-C8	0.0009
C13-H16	1.0825	C3-C8-H7	119.511	C1-C2-C18-H22	0.0217
C17-H19	1.0904	C3-C8-C13	121.3946	C1-C2-C18-H23	-120.233
C17-H20	1.0932	H7-C8-C13	119.0944	C1-C2-C18-H24	120.2719
C17-H21	1.0932	C4-C9-C12	121.0907	C3-C2-C18-H22	180.019
C18-H22	1.0868	C4-C9-H14	118.5163	C3-C2-C18-H23	59.7642
C18-H23	1.0939	C12-C9-H14	120.393	C3-C2-C18-H24	-59.7308
C18-H24	1.0939	C9-C12-C13	119.7583	C2-C3-C4-C5-	0.0004
		C9-C12-H15	120.3904	C2-C3-C4-C9	-180.001
		C13-C12-H15	119.8513	C8-C3-C4C-C5	180.0013
		C8-C13-C12	120.5192	C8-C3-C4-C9	-0.0001
		C8-C13-H16	119.8559	C2-C3-C8-H7	0.0011
		C12-C13-H16	119.6249	C2-C3-C8-C13	180.0012
		C1-C17-H19	110.4939	C4-C3-C8-H7	-179.9999
		C1-C17-H20	112.092	C4-C3-C8-C13	0.0002
		C1-C17-H21	112.0962	C3-C4-C5-C6	0.0011
		H19-C17-H20	107.3269	C3-C4-C5-H10	179.9994
		H19-C17-H21	107.3299	C9-C4-C5-C6	180.0026
		H20-C17-H21	107.2478	C9-C4-C5-H10	0.0008
		C2-C18-H22	112.011	C3-C4-C9-C12	-0.0005
		C2-C18-H23	111.465	C3-C4-C9-H14	-179.9997
		C2-C18-H24	111.4622	C5-C4-C9-H12	-180.0019
		C2-C18-H24	107.3121	C5-C4-C9-H14	-0.0011
		H22-C18-H24	107.31	C4-C5-C6-C1	-0.0022
		H23-C18-H24	107.0099	C5-C4-C6-H11	179.9992
				H10C5-C6-C1	179.9996
				H10-C5-C6-H11	0.001
				C3-C8-C13-C12	0.0002
				C3-C8-C13-H16	-179.9998
				H7-C8-C13-C12	180.0003
				H7-C8-C13-H16	0.0004
				C4-C9-C12-C13	0.0008
				C4-C9-C12-H15	180.0013
				H14-C9-C12-C13	180.0001
				H14-C9-C12-H15	0.0005
				C9-C12-C13-C8	-0.0007
				C9-C12-C13-H16	179.9992
				H15-C12-C13-C8	179.9988
				H15-C12-C13-H16	-0.0013

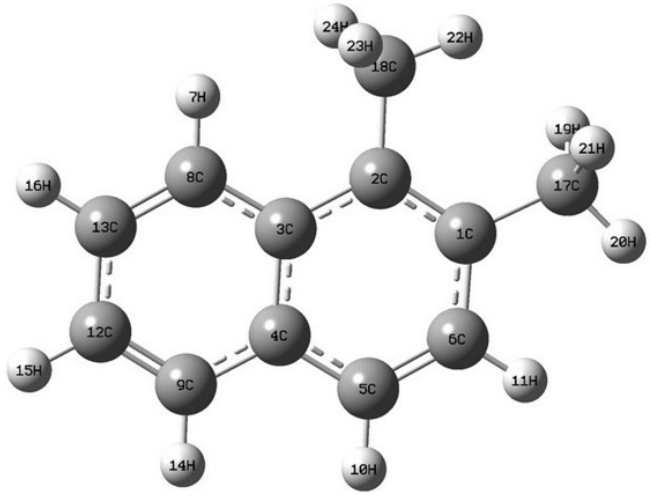

Fig. 1. Optimized structure of 1,2-dimethylnaphthalene with numbering

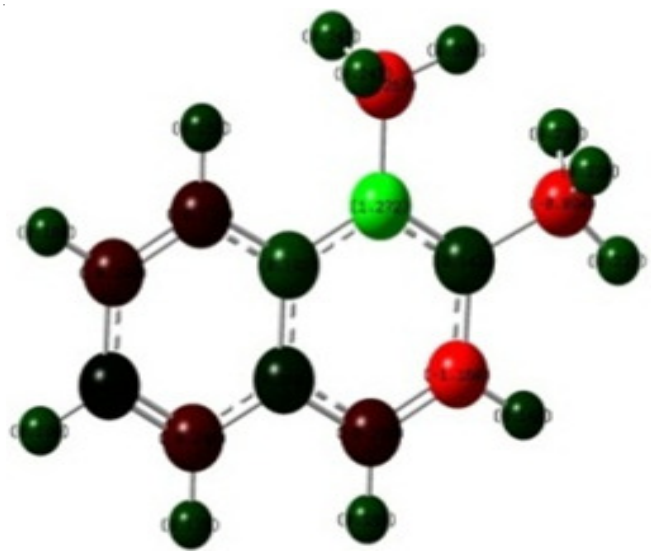

Fig. 2. Mullikan charge distribution of 1,2-dimethylnaphthalene

the single bond [8]. The calculated bond length between the ring carbon and methyl carbon *i.e.* C_1-C_{17} and C_2-C_{18} are found to be 1.514 and 1.516 Å, respectively, which are consistent with the values reported in the literature [9].

The methyl group attached with the ring is found to be altered the ideal bond angle of 120°. Here the bond angle C_2-C_1-C_{17} and C_1-C_2-C_{18} are 122.3° and 121.3°, respectively. This is due to the overcrowding of these bulky methyl groups present in the vicinity of the reaction center, interfere with each other in space and orient them to minimize the strain imposed due to electron repulsion. This steric effect, which arises due to the spatial interaction, has greater influence on physical properties, chemical reactivity, geometric size and shape of the molecule [10]. The other bond angles, especially C_2-C_3-C_8, C_5-C_4-C_9, C_1-C_6-C_5, C_5-C_8-C_{13} and C_4-C_9-C_{12} are 122°, 121.7°, 121.8° and 121.3° respectively, which are slightly higher than the ideal bond angle, owing to the localized π bonds in poly aromatic hydrocarbon [9].

Most of the experimental data are found to be consistent with the computed geometric parameters except the parameter of the methyl substituents [11].

Mullikan charge distribution: Mullikan population analysis computes charges by assuming the overlap between two orbitals shared equally. Generally, it is calculated by determining the electron population of each atom as defined by the basis function. The study of distribution of charges on an atom plays a vital role in the application of the molecular system based on atomic charge, dipole moment, molecular polarizability, electronic structure and acid-base behaviour of the system [12]. The Mullikan population analysis found to be very effective for small basis sets. As the estimation of Mullikan charge for large basis set and with the inclusion of diffuse functions is inaccurate, the Mullikan charge distribution is highly dependent on the basis set and the method of calculation.

The diagrammatic representation of the DFT results of the Mullikan charge distribution analysis and the distribution of charges on each atom in the molecule is depicted in Fig. 2 and the corresponding parameters are presented in Table-2. The Mullikan population analysis calculated in HF and DFT methods are compared and shown in Fig. 3. In the compound under investigation, all the hydrogen atoms both in the substituent and in the ring have a positive charge. In the ring, carbon atom has high negative atomic charge, this shows the electronegativity behaviour of the atom and in turn the substitution is electrophilic in nature [13]. The C_2 atom acquires positive charge, increase the stability of structure [14].

TABLE-2
MULLIKAN'S ATOMIC CHARGE OF 1,2-DIMETHYL-NAPHTHALENE BASED ON HF AND B3LYP METHODS

Atoms	HF 6-311++G	DFT 6-311++G
1C	2.045699	0.142547
2C	0.9206	1.272314
3C	0.389517	0.19176
4C	0.723086	0.067963
5C	-0.40495	-0.197607
6C	-0.36387	-1.160293
7H	0.332196	0.150662
H8	0.385797	-0.171684
9C	-0.76889	-0.240118
10C	-0.42068	0.189269
11H	0.328493	0.149428
12H	0.33634	0.014047
13C	-1.72886	-0.203991
14C	0.584435	0.175138
15H	0.371105	0.190117
16H	0.302971	0.188577
17C	-1.7632	-0.893921
18C	-1.8381	-1.267461
19H	0.262024	0.237963
20H	0.261834	0.231461
21H	0.385414	0.23794
22H	0.260385	0.202431
23H	0.260287	0.246693
24H	0.30723	0.246766

Spectral assignment: It is of interest to study the spectral features of the compound and to correlate with the vibrational structure of molecule. 1,2-Dimethylnaphthalene has 24 atoms and hence 66 normal modes of vibration among them 45 in-plane modes and 21 are out-of-plane modes. The detailed analysis of the fundamental vibrational modes, along with the calculated IR and Raman frequency and normal modes description are presented in Table-3. In present study, we have followed multiple scaling factors for both the methods. After scaling,

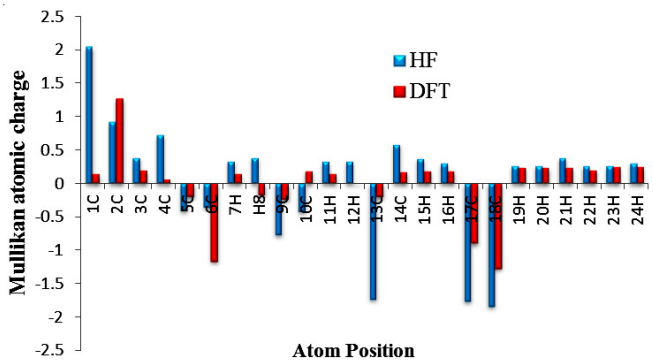

Fig. 3. Histogram of calculated Mullikan charge distribution of 1,2-dimethylnaphthalene

the deviation from the experimental values are less than 10 cm^{-1} with few exceptions.

C-H vibrations: In heteroaromatic compound, the C-H stretching vibrations generally lies in the region 3100-3000 cm^{-1} [15]. Accordingly the title compound has C-H symmetric and antisymmetric vibrations observed at 3050, 3035, 3000 cm^{-1} in FTIR and 3184, 3040, 3006, 3000 cm^{-1} in FT-Raman spectra. The C-H in-plane vibrations appears in the range of 1300-1000 cm^{-1} in the substituted benzene [16], the bands are observed at 1302, 1251, 1219 cm^{-1} and the C-H out-of-plane bending vibra-tions are well identified in 964, 949, 937, 925, 876 cm^{-1}.

C-C vibrations: The aromatic C-C ring vibration occurs in the range of 1625-1430 cm^{-1} especially stretching [17]. The FT-IR bands at 1630, 1602, 1565, 1532, 1527, 1495, 1430 and 1415 are assigned to CC stretching vibrations and the corresponding theoretically computed wavenumbers are at 1627, 1604, 1575, 1532, 1519, 1475, 1457 and 1386 cm^{-1} in B3LYP method. The frequency observed in 1253, 1223 and 1203 cm^{-1} in IR are assigned as C-C in-plane bending vibrations which appears in combination with the CH bending vibrations [18]. The vibrations at 477 and 270 cm^{-1} are identified as ring deformation vibrations are found in accordance with Pouchaname *et al.* [19]. The C-C-C in plane bending and out-of-plane bending vibrations lies

TABLE-3
VIBRATIONAL ASSIGNMENTS OF FUNDAMENTAL OBSERVED FREQUENCIES AND CALCULATED FREQUENCIES OF 1,2-DIMETHYL NAPHTHALENE USING HF/6-311++g AND B3LYP/6-311++g METHODS

Mode	Species	Observed frequency (cm^{-1})		Calculated frequency (cm^{-1})			IR intensity	Raman intensity	Vibrational assignments[a]
		FT-IR	FT-Raman	Unscaled	Scaled HF	Scaled DFT			
1	A'		3185	3195	3168	3153	23.11	189.14	ν_s(CH)
2	A'	3050	3054	3180	3047	3037	39.86	180.41	ν_s(CH)
3	A'		3040	3171	3039	3028	44.86	167.41	ν_{as}(CH)
4	A'	3035		3162	3028	3020	11.67	119.49	ν_{as}(CH)
5	A'		3006	3150	3017	3008	4.81	69.3	ν_s(CH)
6	A'	3000	3000	3147	3014	3005	5.52	29.77	ν_{as}(CH)
7	A'		2975	3128	2983	2972	24.02	63.96	ν_{as}(CH)(CH_3)
8	A'	2955		3091	2941	2952	25.1	56.48	ν_{as}(CH)(CH_3)
9	A'	2921		3061	2920	2923	18.5	84.86	ν_{as}(CH)(CH_3)
10	A'	2858	2850	3053	2817	2839	27.72	85.86	ν_s(CH)(CH_3)
11	A'	2750	2745	3010	2747	2739	47.48	414.93	ν_s(CH)(CH_3)
12	A'	2732	2730	3008	2714	2737	26.67	57.04	ν_s(CH)(CH_3)
13	A'	1630		1660	1632	1627	3.57	15.71	ν(C=C)
14	A'	1602	1605	1637	1601	1604	7	9.8	ν(C=C)
15	A'	1565	1585	1607	1545	1575	3.2	58	ν(C=C)
16	A'		1532	1554	1504	1523	18.24	2.17	ν(C-C)
17	A'	1527		1550	1498	1519	0.08	7.24	ν(C=C)
18	A'	1495	1497	1545	1460	1475	8.21	9.72	ν(C-C)
19	A'		1459	1528	1446	1459	5.05	23.05	ν(C=C)
20	A'	1430	1430	1528	1430	1436	19.58	18.98	ν(C-C)
21	A'	1415	1420	1507	1413	1417	1.16	22.71	ν(C-C)
22	A'		1390	1474	1378	1386	0.87	21.34	ν(C-C)
23	A'	1370	1372	1457	1371	1370	5.55	28.93	ν(C-C)
24	A'		1365	1449	1364	1362	3.85	26.4	β(CH) + δCH(CH_3)
25	A'	1330		1418	1337	1333	10.74	3.28	β(CH) + δCH(CH_3)
26	A'	1295		1400	1283	1302	1.1	235.94	β(CH)
27	A'	1253	1245	1375	1255	1251	1.2	1.02	β(CH) + βCC
28	A'	1223	1220	1311	1223	1219	1.87	3.07	β(CH) + βCC
29	A'	1203	1196	1270	1195	1194	2.82	2.5	β(CH) + γCCC+ βCC
30	A'	1170	1170	1245	1160	1170	3.21	3.66	νC-CH_3
31	A'	1156	1150	1221	1151	1148	4.69	2.75	νC-CH_3
32	A'	1136	1136	1204	1128	1132	2.08	0.46	βC-C
33	A'	1095		1193	1092	1086	0.89	5.16	βCH(CH_3) + β(C-C)
34	A'	1065		1110	1056	1055	3.41	0.57	βCH(CH_3) + ρCH_3
35	A'		1050	1096	1049	1047	0.51	0.01	βCH(CH_3) + γCCC + ρCH_3
36	A'	1025	1020	1092	1006	1016	0.96	4.82	βCH(CH_3)

37	A'	1010		1070	1004	1006	1.79	0.87	$\beta CH(CH_3)$
38	A"	985		1047	977	984	5.99	34.74	$\beta CH(CH_3)$
39	A"		964	1027	968	965	8.42	1.23	γCH
40	A"	949		1015	934	944	0.33	0.31	γCH
41	A"	937	937	1003	933	933	2.28	0.02	$\gamma CH + \beta CCC$
42	A"	925		987	913	918	0.87	1.14	$\gamma CH + \beta CCC$
43	A"		876	892	867	874	1.54	3.74	γCH
44	A"	854	845	888	855	848	5.37	0.01	γCH
45	A'	815		879	809	817	0.05	6.03	$\gamma CH(CH_3) + \gamma CCC$
46	A'		790	842	781	791	66.81	0.02	$\gamma CH(CH_3)$
47	A"		738	780	738	733	27.88	0.5	$\gamma CH(CH_3)$
48	A"	719	725	766	706	720	14.59	0.01	$\gamma CH(CH_3)$
49	A"	713		744	694	711	1.19	5.6	$\gamma CH(CH_3)$
50	A"	672		698	669	667	0.74	24.14	$\gamma CH(CH_3)$
51	A'		627	664	620	624	1.73	0.35	γCH
52	A'		560	590	563	555	0.65	13.09	γCH
53	A'	520	510	555	523	522	8.93	0.19	γCCC
54	A'	505		534	505	502	0.17	4.21	γCCC
55	A"	479	467	525	479	478	0.53	0.14	γCCC
56	A"	459		477	457	453	1.66	4.14	$\beta C\text{-}CH_3$
57	A"	420	430	445	416	425	0.35	15.54	$\beta C\text{-}CH_3$
58	A"	387		431	397	392	3.69	1.53	$\gamma C\text{-}CH_3$
59	A'	332		353	331	332	0.15	0.26	$\gamma C\text{-}CH_3$
60	A'	290		305	286	287	2.88	0.95	γCCC
61	A"	272	270	285	273	268	0.88	1.44	Rasymd
62	A"	213		225	212	212	3	0.23	tCH_3
63	A"	156		163	159	153	0.18	1.49	tCH_3
64	A"	140	148	149	145	140	0.56	0.05	tCH_3
65	A"	120		127	119	119	0.75	1.22	tCH_3
66	A"	96		102	97	96	0.52	0.76	τCH_3

[a]Abbreviations: ν_s – Symmetric stretching; ν_{as} -Asymmetric stretching; γ -Out-of-plane bending; β -inplane bending ; δ -Scissoring ; ρ -rocking ; τ-torsion ; t -twisting ; Rasymd -ring asymmetric deformation.

in the frequency region below 1000 cm^{-1} [20] and in line with this fact frequencies at 937 cm^{-1} and 925 cm^{-1} and at 505 cm^{-1} and 420 $cm^{-1}$are identified as C-C-C in plane bending and out-of-plane bending vibrations, respectively.

Methyl group vibrations: The aromatic C-H stretching vibrations generally occur at (3100-3000 cm^{-1}) but the methyl C-H stretching occurs at lower frequency than this [21]. The symmetric and antisymmetric stretching mode vibrations of the methyl group are expected around 2870 and 2980 cm^{-1}, respectively [22]. For 1,2-dimethylnaphthalene, sharp peaks found at 2858, 2750, 2732 cm^{-1} in IR are assigned to symmetric stretching and 3975, 2955, 2921 cm^{-1} are assigned to antisymmetric stretching modes. These assignments were well supported by the animations of the Gauss view 05.The band at 1095 and 985 cm^{-1} are assigned to CH_3 in-plane bending vibrations while the band at 815 and 672 cm^{-1} are assigned to CH_3 out-plane bending vibrations [23].

For most of the ringed compounds, the asymmetric scissoring vibrations appear in a constant range from 1460 to 1400 cm^{-1} but for 1,2-dimethylnaphthalene, the vibration observed at 1330 cm^{-1} in IR is assigned as scissoring vibrations, it may be due to the influence of the atoms adjacent to methyl group as indicated by Alpert *et al.* [24]. The CH_3 rocking vibrations are found at 1065 cm^{-1} in IR and 1050 cm^{-1} in Raman and the counterpart DFT vibrations are 1092 and 1056 cm^{-1}. In the lowest frequency region 212, 153, 140 and 119 cm^{-1} are assigned to CH_3 twisting modes and CH_3 torsion is assigned at 96 cm^{-1}.

C-CH_3 vibrations: As there are two methyl groups attached to the naphthalene ring, two C-CH_3 stretching is identified at 1170 and 1150 cm^{-1} [25]. The C-CH_3 vibrations usually combine with C-H bending vibrations [26], according to which C-CH_3 in-plane bending vibrations occurs at 459 and 420 cm^{-1} and the out of plane vibrations occurs at 387 and 332 cm^{-1} [26].

Frontier molecular orbital: As HOMO is the highest occupied orbital it is energetically easy to remove the electrons from this orbital and the LUMO is the lowest unoccupied orbital which is energetically ready to accept the electron into the orbital. The energies of HOMO, LUMO and their orbital energy gaps are calculated using B3LYP/6-311++G method are illustrated in Fig. 4. The Frontier molecular orbital analysis shows the occurrence of charge transfer with in the molecule. Further, this charge transfer implies an electron density transfer from the substituted methyl groups to naphthalene ringed carbon. As methyl groups are electron donating, it increases the electron density of the naphthalene ring and thereby speeds up the electrophilic substitution and making the ring highly reactive. The largest interaction occurs, when the HOMO and LUMO are closest in energy. It is therefore evident that the frontier molecular orbital plays a prominent role in governing chemical reactivity of the molecule.

It has been revealed that the gap between HOMO and LUMO energy levels is an important stability index [27,28]. Furthermore, the large gap in energy implies high stability and the small gap in energy represents low stability. The molecules

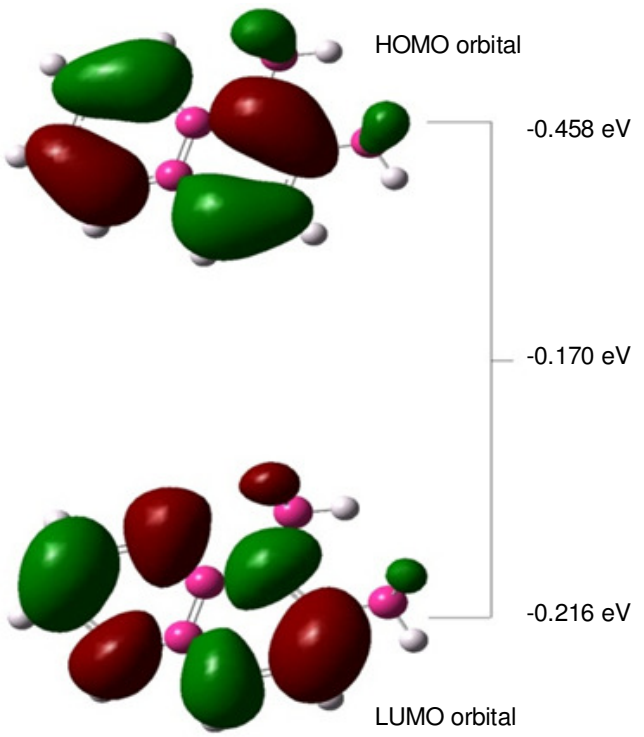

Fig. 4. Frontier molecular orbital of 1,2-dimethylnaphthalene

with high stability index are less reactive in nature, where the molecules with a lower stability are highly reactive [29,30]. Pearson showed that HOMO and LUMO energy gap represents the global hardness of the compound, increase in hardness increases the stability while decrease in hardness decreases the stability of the molecule [31]. Moreover, the hardness and electronegativity is extensively used to predict the aromatic nature of organic compounds and it is also possible to establish an absolute scale of acidity or basicity of the compound. The energy of HOMO orbital and LUMO orbital, chemical hardness and chemical softness and dipole moment are displayed in Table-4.

TABLE-4
CALCULATED ENERGY VALUES OF
1,2-DIMETHYLNAPHTHALENE

Parameters	B3LYP	HF
E_{HOMO} (ev)	-0.0458	-0.28476
E_{LUMO} (ev)	-0.21641	0.03857
ΔEHOMO-LUMO (ev)	-0.17061	0.32334
Chemical hardness	0.085305	0.161665
Chemical softness	11.72264	6.18563
Dipole moment (Debye)	0.7551	0.703

Molecular electrostatic potential energy surface maps: The electrostatic potential maps are very useful three dimensional diagrams, which is an indication of the net electrostatic effect produced at that point by total charge distribution of the molecule and correlates with the dipole moment, electronegativity and partial charge distribution of the molecule. It enable us to visualize the reactive sites of a molecule which are invaluable in predicting the behaviour of the complex molecules [32]. In molecular electrostatic potential surface (MEPS) map, red colour indicates the areas of low potential energy, which are characterized by an abundance of electrons and shows a higher electronegativity further the blue colour indicates the area of high potential energy, characterized by a relative absence of electrons [33].

Accordingly, for the compound under investigation the red colour, representing the higher electronegativity lies over the naphthalene ring and the areas of high potential energy are blue in colour situated on the methyl group of dimethylnaphthalene. This clearly indicates that the electrophilic attack of methyl substituent over the naphthalene ring system. As the substitutes are electron donating, it makes the naphthalene ring electron rich and hence the molecule is highly reactive in nature. The outer area of the map are blue in colour representing the hydrogen atoms and non-red or green region in the map indicates the intermediary potential energy. Here, we can see the greater region of intermediary potential, which indicates the smaller electronegativity difference. The MEPS map (Fig. 5) represents the first substitution directs the incoming second methyl group to *ortho*-position rather than *para* and *meta*-positions. The electronegativity difference is a key to determine the nature of the chemical bonds.

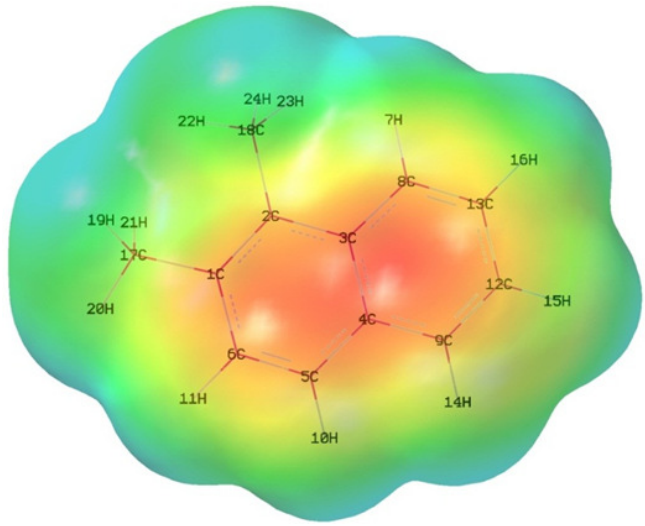

Fig. 5. Molecular electrostatic potential surface map of 1,2-dimethylnaphthalene

Non-linear optical properties: NLO materials have non-linear response to the electric field associated with the light, leading to a variety of optical phenomena such as generations of new light frequencies or alteration of material properties. These NLO properties are much significant for the emerging technologies such as telecommunication, signal processing and optical interaction [34,35].

The non-linear optical response of dimethylnaphthalene in an electric field was calculated using DFT/B3LYP with 6-311++G basis set. The mean polarizability (α), first order hyperpolarizability (β) dipole moment (μ) and anisotropic polarizability (Δα) are defined as given by Sundaraganesan *et al.* [36]:

$$\mu = \mu_x^2 + \mu_y^2 + \mu_z^2$$

$$\alpha = \frac{\alpha_{xx} + \alpha_{yy} + \alpha_{zz}}{3}$$

$$\Delta\alpha = 2^{1/2}\left\{(\alpha_{xx}-\alpha_{yy})^2+(\alpha_{yy}-\alpha_{xx})^2+6\alpha_{xx}^2\right\}^{1/2}$$

First order hyperpolarizability is a third rank tensor that can be described by 3 × 3 × 3 matrix. The 27 components of 3D matrix can be reduced to 10 components due to Kleimman symmetry [37]. The output of Gaussian 09w provides 10 components of this matrix, as β_{xxx}, β_{xxy}, β_{xyy}, β_{yyy}, β_{xxz}, β_{xyz}, β_{yyz}, β_{xzz}, β_{yzz}, β_{zzz}, respectively. The first order hyperpolarizability can be calculated using the equation:

$$\beta_z = \left(\beta_x^2+\beta_y^2+\beta_z^2\right)^{1/2}$$

where, $\beta_x = \beta_{xxx} + \beta_{xyy} + \beta_{xzz}$, $\beta_y = \beta_{yyy} + \beta_{xxy} + \beta_{yzz}$, $\beta_z = \beta_{zzz} + \beta_{xxz} + \beta_{yyz}$.

The urea is one of the popular molecular systems used to compare the NLO properties of the organic compounds. Therefore, it is used as a threshold value for the comparison of calculate α and β of 1,2-dimethylnaphthalene and are found to be 20.7415×10^{-24} and 34.049×10^{-30} esu respectively (Table-5), which are greater than those of $\alpha = 9.68774 \times 10^{-24}$ esu and $\beta = 7.803 \times 10^{-30}$ esu values of urea obtained by DFT/B3LYP with 6-311++ basis set [38]. Since the values of polarizability and hyperpolarizability (β) of Gaussian 09w output are reported in atomic units, the theoretically calculated values have been converted into electrostatic units as (α; 1 a.u. = 0.1482×10^{-24} esu and β; 1 a.u. = 8.6393×10^{-33} esu). The first hyperpolarizability of the compound is almost double than the magnitude of urea.

TABLE-5
CALCULATED VALUES OF HYPERPOLARIZABILITIES

Parameters	DFT/B3LYP (6-311++g) (in e.s.u. × 10^{-30})
β_{xxx}	545.1295
β_{xxy}	-468.15630
β_{xyy}	359.40409
β_{yyy}	-18.00233
β_{xxz}	-6.928408
β_{xyz}	2.9138936
β_{yyz}	7.4972779
$\beta_{xzz,}$	179.10014
β_{yzz}	-350.3279
β_{zzz}	-15.91575

It is noticed that, in β_{xxy} direction the first hyperpolarizability is higher and subsequently delocalization of the electron cloud is more in that direction. The domination of a particular component indicates a substantial delocalization of charges in those directions. The maximum β values may be due to π-electron cloud movement from donor to acceptor which makes the molecule highly polarized and the intramolecular charge transfer is possible. The dipole moment in a molecule is an important property that is mainly used to study the intermolecular interactions involving non-bonded type dipole-dipole interaction.

Molecular thermodynamics: Thermodynamic properties such as molar heat capacity, entropy, zero point vibration energy (ZPVE), rotational constant, thermal energy are the measure of the average energy of the translational, rotational and vibrational motions of the particle constituent. They have been obtained from *ab initio* HF and DFT methods using 6-311++g basis set at 298.15 K and at 1 atm pressure is listed in Table-6. The values are calculated for single non-interacting molecule in vacuum, which apply only for an ideal gas. The approximations can introduce some errors depending on the system being studied is non-ideal.

TABLE-6
CALCULATED THERMODYNAMICAL PARAMETERS OF 1,2-DIMETHYLNAPHTHALENE

Parameters	RHF/6-311++G	B3LYP/6-311++G
Zero point energy (Kcal/Mol)	136.32782	127.7416
Entropy (cal/mol-kelvin)		
Translational	41.045	41.045
Rotational	30.344	30.382
Vibrational	22.516	25.209
Total	93.905	96.636
Rotational temperature (Kelvin)		
	0.09063	0.08943
	0.03761	0.03715
	0.02676	0.02643
Rotational constants (GHZ)		
	1.88845	1.86335
	0.78366	0.77416
	0.55759	0.55065
Thermal energy (kcal/mol)		
Translational	0.889	0.889
Rotational	0.889	0.889
Vibrational	140.374	132.227
Total	142.151	134.005
Molar capacity at constant volume (kcal/mol-kelvin)		
Translational	2.981	2.981
Rotational	2.981	2.981
Vibrational	31.084	34.198
Total	37.045	40.16

Generally, the dependence of thermodynamic parameters with the temperature is very important to study. Since, it affects the physical and chemical properties of the molecule. The properties such as entropy, enthalpy and heat capacity have direct relation with the temperature [39]. The correlation between these thermodynamic parameters with the temperature are plotted and fitted by quadratic equations where the fitting factors (R^2) are found to be less than 1 and the corresponding correlation equations are also presented.

$$C_p = -1.675 + 0.1485T - 5 \times 10^{-5}$$

$$\Delta H = 137.32 - 0.4 \times 10^{-3}T - 5 \times 10^{-5} T^2$$

$$S = 51.703 + 0.1497T - 2 \times 10^{-5} T^2$$

The values of the thermodynamic parameters increases linearly with respect to the temperature ranging from 100 to 1500 K at constant volume and pressure are due to the enhancement of molecular vibrations (Table-7). All these thermodynamic data are very useful in providing information's for future studies and to determine the direction of chemical reactions according to the second law of thermodynamics [40]. As expected DFT/B3LYP gives slightly lower value (127.7416 kcal/mol) than HF (136.32782 kcal/mol) method. This difference is mainly due to the approximations that are imposed in Hatree Fock than DFT.

TABLE-7
TEMPERATURE DEPENDENCE OF THERMODYNAMIC PARAMETERS

Temp. (K)	ΔH (kcal mol^{-1})	C_p (cal mol^{-1} K^{-1})	S (cal mol^{-1} K^{-1})
100	137.2	13.702	66.722
200	139.12	24.545	80.956
300	142.22	37.24	94.14
400	146.59	50.067	107.208
500	152.194	61.718	120.105
600	156.19	71.669	132.626
700	158.87	80.007	144.625
800	166.47	87.006	156.044
900	174.835	92.926	166.877
1000	183.84	97.969	177.145
1100	203.41	102.292	186.88
1200	213.829	106.013	196.117
1300	224.59	109.23	204.892
1400	235.661	112.019	213.238
1500	246.98	114.447	221.181

Conclusion

A complete vibrational analysis of haramonic frequencies of the optimized molecular structure of 1,2-dimethylnaphthalene has been carried out and reported for the first time based on the quantum mechanical approach by HF and DFT calculations. The optimized geometrical structure shows a little distorsion due to the sterric hindrance between substituted methyl groups in *ortho*-position, further the optimized structural parameters are compared with the experimental XRD data and found to be consistent with the literature. The Mullikan atomic charge distribution shows that the substitution is electrophilic is nature. From the molecular electrostatic potential energy surface map, the negative potential lies over the ring and the positive potential are around methyl substituents and hydrogen atoms. This indicates the electrophilic attack of methyl group and this fact is well supported by frontier molecular orbital analysis. From the polarizability and hyperpolarizability results of the title compound, it is found that the value of first hyperpolarizability is double than the magnitude of urea and hence, it can be used for NLO applications. All the thermodynamic parameters at different temperatures are also studied and reported.

REFERENCES

1. R. Alexander, R. Kagi and P. Sheppard, *Nature*, **308**, 442 (1984); https://doi.org/10.1038/308442a0.
2. V. Librando and S. Fazzino, *Chemosphere*, **27**, 1649 (1993); https://doi.org/10.1016/0045-6535(93)90146-V.
3. F. Castelli, V. Librando and M. Sarpietro, *Environ. Sci. Technol.*, **36**, 2717 (2002); https://doi.org/10.1021/es010260w.
4. A. Becke, *J. Chem. Phys.*, **98**, 5648 (1993); https://doi.org/10.1063/1.464913.
5. C. Lee, W. Yang and R. Parr, *Phys. Rev. B*, **37**, 785 (1988); https://doi.org/10.1103/PhysRevB.37.785.
6. M.J. Frisch, *et al*., Gaussian09, Revision B.01, Gaussian Inc., Pittsburgh, PA (2009).
7. Y. Tantirungrotechai, K. Phanasant, S. Roddecha, P. Surawatanawong, V. Sutthikhum and J. Limtrakul, *J. Mol. Struct. THEOCHEM*, **760**, 189 (2006); https://doi.org/10.1016/j.theochem.2005.12.007.
8. L. Pauling, The Nature of Chemical Bond and Structure of Molecules and Crystals: An Introduction to Modern Structural Chemistry, Cornell University Press, California, edn 3 (1960).
9. V. Pouchaname, R. Madivanane and A. Tinabaye, *Adv. Mater. Res.*, **584**, 371 (2012); https://doi.org/10.4028/www.scientific.net/AMR.584.371.
10. K.G. Bothara, Organic Pharmaceutical Chemistry, Nirali Prakashan, edn 8 (2008).
11. A. Welzel, A. Hellweg, I. Merke and W. Stahl, *J. Mol. Struct. THEOCHEM*, **215**, 58 (2002); https://doi.org/10.1006/jmsp.2002.8600.
12. I. Sidir, Y.G. Sidir, M. Kumalar and E. Tasal, *J. Mol. Struct*., **964**, 134 (2010); https://doi.org/10.1016/j.molstruc.2009.11.023.
13. C. MacLean and E.L. Mackor, *Mol. Phys.*, **3**, 223 (2006); https://doi.org/10.1080/00268976000100271.
14. V.P. Saxena, Complete Course in ISC Chemistry, Pitamar Publishing Company Pvt. Ltd., Educational Publishers, New Delhi, vol. I (2009).
15. D.N. Sathyanarayana, Vibrational Spectroscopy: Theory and Applications, New Age International (P) Ltd Publishers, New Delhi, edn 2 (2004).
16. V. Pouchaname, R. Madivanane, A. Tinabaye and K.B. Santhi, *Struct. Chem. Commun.*, **2**, 129 (2011).
17. G.Varsanyi, Vibrational Spectra of Benzene Derivatives, Academic Press, New York, London, P. 24 (1969).
18. M. Silverstein, G.C. Basseler and C. Morill, Spectrometric Identification of Organic Compounds, Wiley, New York (1981).
19. V. Pouchaname, R. Madivanane, A. Tinabaye and K.B. Santhi, *Struct. Chem. Commun.*, **3**, 158 (2012).
20. V.R. Dani, Organic Spectroscopy, Tata-MacGraw Hill Publishing Company, New Delhi, India (1995).
21. N. Sundaraganesan, C. Meganathan and M. Kurt, *J. Mol. Struct.*, **891**, 284 (2008); https://doi.org/10.1016/j.molstruc.2008.03.051.
22. J.H.S. Green, D.J. Harrison and W. Kynaston, *Spectrochim. Acta A*, **27**, 807 (1971); https://doi.org/10.1016/0584-8539(71)80159-9.
23. B.C. Smith. Infrared Spectral Interpretation: A Systematic Approach, CRC Press (1998).
24. N.L. Alpert, W.E. Keiser and H.A. Szymanski, IR: Theory and Practice of Infrared Spectroscopy, Plenum/Rosetta edition, edn 2 (1973).
25. M. Dien, Introduction to Modern Vibrational Spectroscopy, Wiley, New York (1993).
26. G. Socrates, Infrared and Raman Characteristic Group Frequencies, John Wiley & Sons, Ltd., Chichester, edn 3 (2001).
27. Z. Zhou and R.G. Parr, *J. Am. Chem. Soc.*, **112**, 5720 (1990); https://doi.org/10.1021/ja00171a007.
28. R.G. Pearson, *J. Org. Chem.*, **54**, 1423 (1989); https://doi.org/10.1021/jo00267a034.
29. J. Aihara, *J. Phys. Chem. Chem. Phys.*, **2**, 3121 (2000); https://doi.org/10.1039/b002601h.
30. X. Liu, T.G. Schmalz and D.J. Klein, *Chem. Phys. Lett.*, **188**, 550 (1992); https://doi.org/10.1016/0009-2614(92)80864-8.
31. R.G. Pearson, *J. Am. Chem. Soc.*, **110**, 2092 (1988); https://doi.org/10.1021/ja00215a013.
32. J.S. Murray and K. Sen, Molecualr Electrostatic Potentials: Concept and Applications, Elsevier. Amsterdam (1996).
33. E.I. Paulraj and S. Muthu, *Spectrochim. Acta A Mol. Biomol. Spectrosc.*, **106**, 310 (2013); https://doi.org/10.1016/j.saa.2013.01.048.
34. Y.-X. Sun, Q.-L. Hao, W.-X. Wei, Z.-X. Yu, L.-D. Lu, X. Wang and Y.-S. Wang, *J. Mol. Struct. THEOCHEM*, **904**, 74 (2009); https://doi.org/10.1016/j.theochem.2009.02.036.
35. V.M. Geskin, C. Lambert and J.-L. Brédas, *J. Am. Chem. Soc.*, **125**, 15651 (2003); https://doi.org/10.1021/ja035862p.
36. N. Sundaraganesan, J. Karpagam, S. Sebastian and J.P. Cornard, *Spectrochim. Acta A*, **73**, 11 (2009); https://doi.org/10.1016/j.saa.2009.01.007.
37. D.A. Kleinman, *Phys. Rev.*, **126**, 1977 (1962); https://doi.org/10.1103/PhysRev.126.1977.
38. D. Pegu, and N.B. Singh, *Int. J. Adv. Res.,* **9**, 531 (2013).
39. J. Ott and J.B. Boerio-Goates: Chemical thermodynamics; Advanced Applications, Academic Press, edn 1 (2000).
40. R. Zhang, B. Du, G. Sun and Y. Sun, *Spectrochim. Acta A*, **75**, 1115 (2009); https://doi.org/10.1016/j.saa.2009.12.067.